

Received March 4, 2020, accepted March 15, 2020, date of publication March 23, 2020, date of current version April 9, 2020.

Digital Object Identifier 10.1109/ACCESS.2020.2982674

# Validity Evaluation of Transformer DGA Online Monitoring Data in Grid Edge Systems

JUN JIA<sup>1,2</sup>, FENGBO TAO<sup>1</sup>, GUOJIANG ZHANG<sup>3</sup>, JIN SHAO<sup>4</sup>,  
XINGHUI ZHANG<sup>4</sup>, AND BO WANG<sup>5</sup>

<sup>1</sup>Research Institute, State Grid Jiangsu Electric Power Co., Ltd., Jiangsu 210036, China

<sup>2</sup>Jiangsu Key Laboratory of Smart Grid Technology and Equipment, School of Electrical Engineering, Southeast University, Jiangsu 210000, China

<sup>3</sup>Equipment Department, State Grid Jiangsu Electric Power Co., Ltd., Jiangsu 210036, China

<sup>4</sup>Equipment Department, State Grid Corporation of China, Ltd., Beijing 100031, China

<sup>5</sup>School of Electrical and Automation Engineering, Wuhan University, Hubei 430072, China

Corresponding author: Bo Wang (whwdwb@whu.edu.cn)

This work was supported in part by the National Key Research and Development Program of China (Technology and Application of Wind Power / Photovoltaic Power Prediction for Promoting Renewable Energy Consumption) under Grant 2018YFB0904200 and in part by the Eponymous Complement S&T Program of State Grid Corporation of China under Grant SGLNDKOOKJJS1800266.

**ABSTRACT** Dissolved gas analysis (DGA) is an important method of predicting transformer faults, and the accuracy of DGA measurements is of great significance to the evaluation of the transformer state in grid edge systems. In actual situations, it is difficult to regularly calibrate online DGA monitoring devices in a uniform way. Therefore, this paper proposes a method based on B-EMD and DBN to evaluate the validity of online DGA monitoring data and optimize the corresponding calibration plan. An analysis of actual DGA signals shows that the method proposed in this paper can effectively diagnose faults and improve the reliability of DGA online monitoring devices.

**INDEX TERMS** Dissolved gas analysis, power transformer, validity evaluation, empirical mode decomposition, deep belief network.

## I. INTRODUCTION

Power transformers are one of the most important pieces of equipment in a power system, and their operation reliability is directly related to the safety of the power system. At present, dissolved gas analysis (DGA) for transformer oil is an effective method of diagnosing transformer defects [1]–[3] and has been widely used to monitor the state of power transformers. However, the service life of a DGA online monitoring device is far lower than that of the power transformer itself, and most DGA online monitoring devices are installed outdoors, where the operating environment is harsh. The accuracy of DGA is greatly reduced because of the dead oil that results from unreasonable oil circuit design, the aging of degassing devices, spectrometer deviations and other factors that lead to invalid data, thus reducing the reliability and confidence of DGA monitoring data.

Currently, it is difficult to regularly calibrate online DGA monitoring devices in a uniform way in actual scenarios due to the complexity of on-site calibration and extensive professional requirements. Therefore, it can be determined whether there are aging or other problems with DGA online

monitoring devices by evaluating the validity of oil chromatography data. In this approach, the calibration and maintenance of high-risk DGA online monitoring devices can be prioritized, which is of important significance for improving the accuracy of DGA state monitoring devices and the operating safety of the power transformer. In the actual operation of a power transformer, the ambient temperature and relative humidity, load, oil temperature and other factors will influence the DGA results both directly and indirectly. Reference [4] found that the DGA signal itself is complex and chaotic and can be obtained by calculating the Lyapunov Index of the signal.

In the literature, there have been a large number of studies on dissolved gas signal analysis, mostly focusing on the diagnosis and analysis of power transformer defects [2], [5]–[8]. Few studies have focused on the accuracy of online devices. Currently, support vector machines are mainly used to improve the accuracy of online DGA signals. Because the corresponding model is too simple and requires offline data for support, this approach is not feasible in practical applications. Reference [9]–[14] uses the fast-MCD robust analysis method to detect outliers in DGA signals based on the Mahalanobis distance. However, the calibration of the Mahalanobis distance is easily affected by

The associate editor coordinating the review of this manuscript and approving it for publication was Xiaokang Wang.

DGA changes in monitoring devices, and such changes in the effectiveness of the DGA online monitoring devices tend to be reflected in the signal of the DGA changes.

Reference [15] decomposes the defects in DGA online devices into five types (i.e., fixed deviation, drift deviation, transformation ratio deviation, precision distortion fault and complete failure defects) to evaluate the effectiveness of DGA data using threshold, variation, and slope criteria, among others. Because of the complexity of DGA signals, however, the methods above tend to cause a large number of false statements and misstatements due to the improper selection of parameters [16]–[20].

Therefore, it is extremely difficult to determine how to reduce the impact of monitoring in the analysis of DGA signals. Therefore, this paper proposes a method based on B-EMD and DBN to evaluate the validity of online DGA monitoring data and optimize the calibration scheme. An analysis of actual DGA signals shows that the method proposed in this paper can effectively diagnose the faults of DGA online monitoring devices and improve device reliability.

## II. INTRINSIC MODEL ANALYSIS OF DGA SIGNAL BASED ON B-EMD

In analyses of DGA signals, most traditional signal processing methods need to predefine the primary functions (such as by Fourier analysis and wavelet analysis). However, the DGA signals collected by online devices are mostly non-stationary signals, and the power spectrum and correlation function are time varying, so it is difficult to select a unified primary function for decomposition.

In 1998, Huang proposed a new signal processing method called empirical mode decomposition (EMD). The core idea of the EMD method is to decompose non-stationary complex signals into series of intrinsic mode functions (IMFs). Each IMF is decomposed based on its own characteristics for the given signals and contains the local characteristics of the signals at different scales. Because it is not necessary to predefine the primary function, the EMD method has high adaptability for non-stationary signals. EMD has been used in signal detection analysis for power equipment [21]–[26].

The calculation process of the standard EMD method is as follows. For input signal  $x(t)$ , search the all the maximum/minimum sequences of  $x(t)$ , that is,  $x_+(t)$  and  $x_-(t)$ . Then, perform three spline interpolations for the maximum/minimum sequences  $x_+(t)$  and  $x_-(t)$  separately before obtaining the upper/lower envelope curves of the original input signal  $x(t)$ , which are expressed as  $e_+(t)$  and  $e_-(t)$ . Next, calculate the mean signal  $m(t)$  through the following formula.

$$m(t) = \frac{e_+(t) + e_-(t)}{2} \quad (1)$$

The quasi-signal  $h(t) = m(t) - x(t)$  must satisfy the following criteria.

1) The difference between the number of zero crossing points and the number of extreme points should be no greater

than one.

$$|\text{count}(e_+(t)) - \text{count}(e_-(t))| \leq 1 \quad (2)$$

2) At any point in the signals studied, the mean value of the upper and lower envelope curves determined by the local maximum and local minimum points should be less than the set threshold SD.

$$SD = \sum_{t=0}^T \frac{[h_{k-1}(t) - h_k(t)]^2}{h_{k-1}^2(t)} \quad (3)$$

3) If the quasi-modal signal  $h(t)$  has the above two conditions,  $h(t)$  is the first IMF component  $IMF_1$  of the original signal. Otherwise,  $x(t) = h(t)$ , and the above steps are repeated.

The key step in this method is obtaining the upper and lower envelope curves of the original signal. The acquisition of the envelope curves is highly dependent on the locations of the extreme points of the input signal and the accuracy of the value information. Therefore, the sampling rate should be much higher than the Nyquist frequency of the signal to obtain stable and accurate EMD results for a group of signals [24]. However, the sampling rate of DGA signals is low, and because of the acquisition error of the devices, DGA signals are chaotic [4], [5], [27]. The extreme points of the signal are often inaccurate. The sampling error will affect the accuracy of the decomposition results, thus reducing the accuracy of the state analysis of the DGA sensors. To address the problem of performing accurate EMD for low-frequency signals, the existing methods mainly consider the interpolation of signals before relocating the extreme points to reduce errors. References [24], [25], [28] reconstructed the original signal based on interpolation, and reference [29] used ascending cosine interpolation to extract the envelope curves of the signals. However, sinc interpolation and ascending cosine interpolation have drawbacks such as a slow convergence speed and boundary distortion, making them difficult to apply in practice [30]–[36].

Therefore, this paper proposes a pretreatment method for DGA signals based on B-spline fitting. Unlike the traditional interpolation algorithm, the B-spline fitting algorithm is characterized by the same performance as a low pass filter and can effectively reduce the effect of chaos and improve the stability of EMD for small sets of DGA data.

Assuming that the original DGA data curve is  $y(t)$ , the fitted curve  $g(t)$  of the B-spline of order  $p$  can be expressed as

$$g(t) = \sum_{j=0}^n c_j B_{j,p}(t) \quad (4)$$

where  $c_j$  refers to the B-spline parameter to be determined and  $B_{j,p}$  refers to the B-spline function of order  $p$ . Assuming that the original DGA monitoring sequence is  $u = \{u_0, u_1, u_2, \dots, u_{n+p}\}$ , the B-spline function  $B_{j,p}$  of order  $p$  can be calculated using the Cox-deBoor recursive

formula [18].

$$B_{j,1}(t) = \begin{cases} 1 & u_j \leq t \leq u_{j+1} \\ 0 & \text{other} \end{cases} \quad (5)$$

$$B_{j,p}(t) = \frac{t - u_j}{u_{j+p-1} - u_j} B_{j,p-1}(t) + \frac{u_{j+p} - t}{u_{j+p} - u_{j+1}} B_{j+1,p-1}(t), \quad (p > 1) \quad (6)$$

The difference between the fitted curve  $g(t)$  of the B-spline method and the original DGA signals is  $\varepsilon(t)$ .

$$\varepsilon(t) = y(t) - g(t) \quad (7)$$

Therefore, the parameters to be determined in B-spline fitting can be obtained by the least squares of  $\varepsilon(t)$ .

$$\begin{aligned} \min |\varepsilon(t)| &= \min (\varepsilon^2(t)) = \min \left( \sum_t (y(t) - g(t))^2 \right) \\ &= \min \left( \sum_t \left( y(t) - \sum_{j=0}^n c_j B_{j,p}(t) \right)^2 \right) \end{aligned} \quad (8)$$

Ideally, assuming the measured signal is a constant value  $\mu$ , the signals measured by the DGA monitoring device should satisfy a normal distribution with  $\mu$  as the mean and  $\sigma$  as the variance (related to the measurement accuracy and aging degree of the DGA device).

The sampling frequency of DGA is generally 1-3 times a day. Because each IMF decomposed by B-EMD can be regarded as a narrow-band signal, and when combined with the actual decomposition effect of B-EMD, the error signals caused by the DGA measuring device are mainly distributed in  $IMF_1$ – $IMF_3$ , as shown in Fig.1.

### III. VALIDITY EVALUATION OF DGA SIGNAL EFFECTIVENESS BASED ON A DBN NETWORK

#### A. CONSTRUCTION OF A VALIDITY EVALUATION NETWORK FOR DGA SIGNALS

A deep belief network (DBN) is a probability-generating model with multiple hidden layers and is used to evaluate the conditional probability of events [37]–[39], such as  $P(\text{Observation} | \text{Label})$  and  $P(\text{Label} | \text{Observation})$ , by establishing a joint probability distribution between Observation and Label. Such networks have already been applied in transformer fault analysis [1], [40], [41], insulator fault analysis [42] and fan fault analysis [43]–[47].

A DBN can pretrain unsupervised labeled samples with a layer-by-layer unsupervised learning algorithm before training labeled samples to obtain a near-optimal solution for the network parameter distribution before fine tuning the data according to the labeled samples to speed up the network training process.

Structurally, the DBN can be viewed as a stack of multiple RBMs as shown in Fig.2.

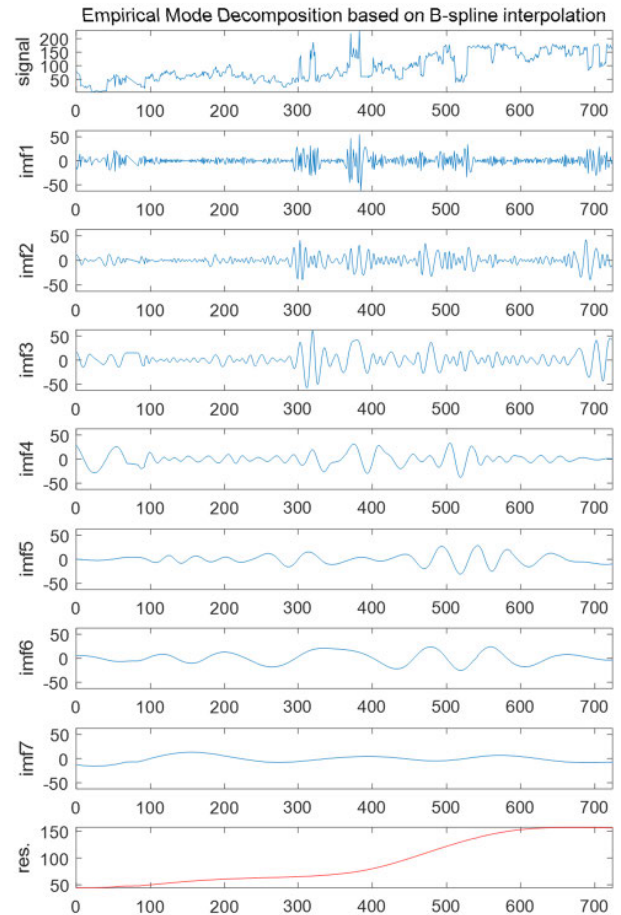


FIGURE 1. Diagram of B-EMD for a DGA Signal.

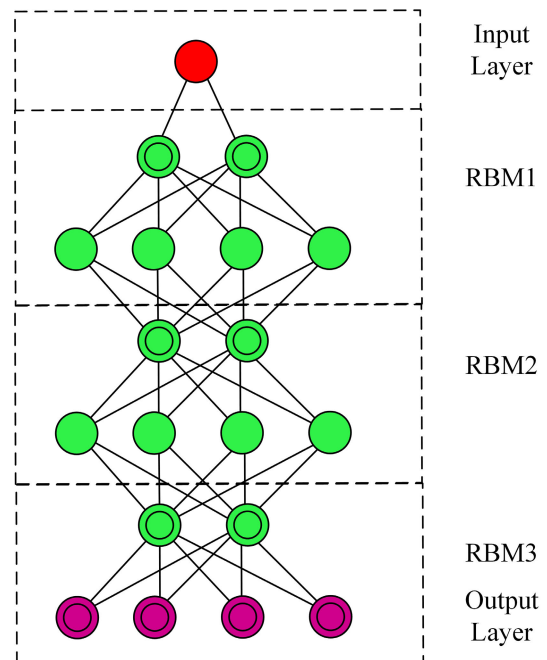


FIGURE 2. DBN network schematic diagram.

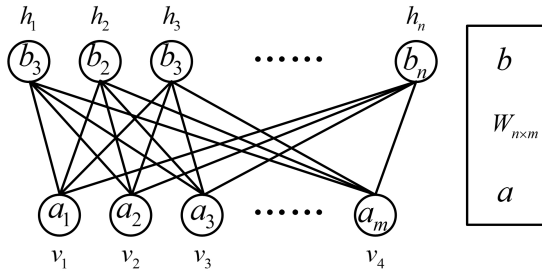


FIGURE 3. RBM structural diagram.

Each RBM unit consists of a visual layer ( $v \in \{0, 1\}^D$ ) and a hidden layer ( $h \in \{0, 1\}^M$ ), where  $D$  and  $M$  refer to the dimensions of time variables with an energy function defined as follows:

$$E(v, h; \theta) = - \sum_{i=1}^D \sum_{j=1}^M W_{ij} v_i h_j - \sum_{i=1}^D b_i v_i - \sum_{j=1}^M a_j h_j \quad (9)$$

where the model parameter  $\theta = \{W, b, a\}$ ,  $W_{ij}$  refers to the weight between node  $v_i$  in the visual layer and node  $h_j$  in the hidden layer,  $a_j$  and  $b_i$  are the bias coefficients of the model.

$$p(v; \theta) = \frac{p^*(v; \theta)}{Z(\theta)} = \frac{1}{Z(\theta)} \sum_h e^{-E(v, h; \theta)} \quad (10)$$

$$Z = \sum_v \sum_h e^{-E(v, h; \theta)} \quad (11)$$

where  $p^*$  is the unnormalized probability function and  $Z(\theta)$  is the partitioning function or normalized constant.

Therefore, a single-layer RBM network can be represented as Fig.3.

Based on EMD and a DBN, the network is divided into three parts: the EMD module, the DBN recognition module and the weighted average module.

Based on B-spline interpolation and the EMD of input information, the first three IMFs  $IMF_1\_IMF_3$  can be obtained. Then, each  $IMF_n (n = 1, 2, 3)$  of five characteristic gases is separately connected to the three independent DBNs. Finally, the output results of the DBNs are entered into the BP network for weighting factor sorting to obtain the final results.

The overall structure diagram of the validity analysis of DGA monitoring data based on B-EMD and DBN DGA is shown in Fig. 4.

**B. TRAINING OF THE VALIDITY EVALUATION NETWORK OF DGA SIGNALS**

**1) SELECTION OF TRAINING SAMPLES**

The training sample data from the validity evaluation network of DGA signals can be divided into unlabeled sample data and labeled sample data.

The unlabeled sample data are mainly derived from the actual DGA online monitoring data after eliminating the intermittent values, zero values, infinite values and other abnormal data.

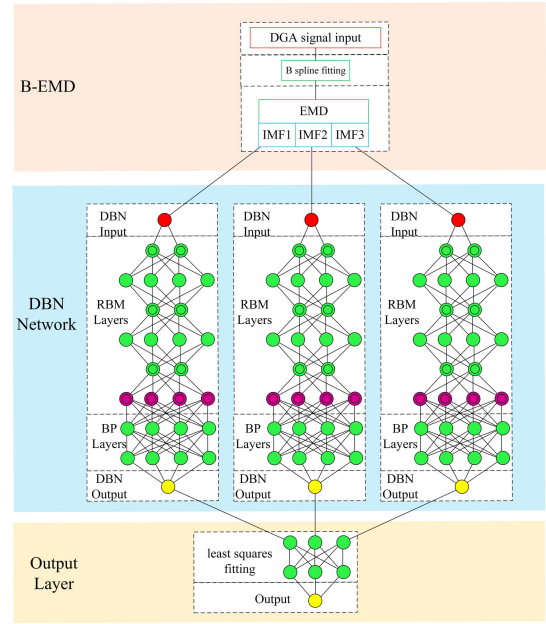


FIGURE 4. Structure diagram of validity analysis of DGA monitoring data based on B-EMD and DBN.

The labeled samples are mainly derived from the online DGA monitoring devices with calibration records and including the following data types:

- The monitoring data from normal transformer DGA and qualified monitoring device calibration (positive samples);
- The abnormal offline testing data from transformer DGA but for the normal calibration of typical devices (positive samples);
- The data for monitoring devices that are not qualified for calibration (negative samples).

**2) PRETRAINING PROCESS OF THE DBN**

According to Formulas (6) - (8), the conditional probability distribution between the node  $v_i$  in the visual layer and the node  $h_j$  in the hidden layer can be expressed as follows.

$$\begin{cases} p(h|v) = \prod_j p(h_j|v) \\ p(v|h) = \prod_i p(v_i|h) \end{cases} \quad (12)$$

$$\begin{cases} p(h_j = 1|v) = \sigma(\sum_i W_{ij} v_i + a_j) \\ p(v_j = 1|h) = \sigma(\sum_i W_{ij} h_i + b_j) \end{cases}, \sigma(x) = \frac{1}{1 + e^{-x}} \quad (13)$$

According to Formulas (7) - (10), the parameter  $\theta$  in the RBM can be obtained by the maximum likelihood function of the edge distribution of  $\theta$  through  $p(c, h; \theta)$ .

$$p(v; \theta) = \frac{1}{Z} \sum_h \exp(-E(v, h; \theta)) \quad (14)$$

The training algorithm of the RBM parameters can be described as follows:

$$\begin{cases} \Delta w_{ij} = \varepsilon (\langle v_i h_i \rangle_{data} - \langle v_i h_i \rangle_k) \\ \Delta b_i = \varepsilon (\langle v_i \rangle_{data} - \langle v_i \rangle_k) \\ \Delta a_i = \varepsilon (\langle h_i \rangle_{data} - \langle h_i \rangle_k) \end{cases} \quad (15)$$

where  $\varepsilon()$  is the learning efficiency function;  $\langle \rangle_{data}$  is the mathematical expectation function of training samples;  $\langle \rangle_k$ ,  $\Delta w_{ij}$ ,  $\Delta b_i$  and  $\Delta a_i$  are the mathematical expectation function, the updating weight and the updating offset after sub-Gibbs sampling  $k$  times for the training samples, respectively [48].

The entire pretraining process of the DBN can be described as follows:

- Train the RBM in the first layer;
- Use the parameters of the hidden layer in the RBM in the second layer as inputs for the Level 2 RBM;
- Train the RBM in the second layer.

The pretraining of the entire DBN can be completed in the same manner.

### 3) FINE-TUNING PROCESS OF THE DBN

After pretraining, the DBN is fine tuned by marking samples. The fine-tuning process is described as follows: the output of the RBM in the last layer of the DBN is taken as the input of the back-propagation network and supervised by the back-propagation algorithm from back to front [31], [49]–[53].

### 4) ENTIRE NETWORK TRAINING PROCESS FOR DGA EFFECTIVENESS EVALUATION

The entire training process can be described in four stages, as shown in Fig. 5.

In stage 1, B-spline interpolation and EMD are conducted on all samples to obtain samples  $IMF_1$ – $IMF_3$ . In stage 2, unlabeled decomposition samples  $IMF_1$ – $IMF_3$  are used to pretrain DBNs 1-3 according to Formulas (12) - (15). In stage 3, the labeled decomposition samples  $IMF_1$ – $IMF_3$  are used to train DBNs 1-3 through the BP algorithm. In stage 4, the labeled samples are diagnosed by the trained DBN, and the output results are used as inputs to train the weighted factor sorting network through the BP algorithm.

## IV. CASE STUDY

To verify the reasonability and validity of the method proposed in this paper, the recognition accuracy of the deep learning model under different feature extraction mechanisms is comparatively analyzed. Moreover, the model structures and training parameters are changed for comparative verification and to obtain the optimal validity evaluation model. Additionally, this paper compares the proposed method with other methods, such as black box testing and multicriteria fusion, to further validate the proposed method.

### A. CASE DESCRIPTION

The current DGA online monitoring devices are expected to detect seven characteristic gases, including  $H_2$ ,  $CH_4$ ,  $C_2H_4$ ,

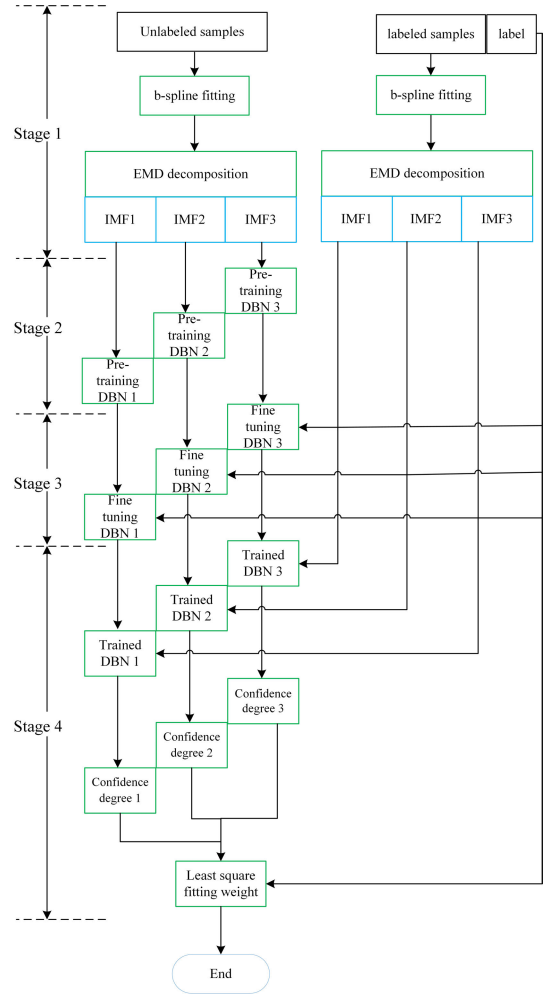


FIGURE 5. Flowchart of DGA signal validity evaluation network training.

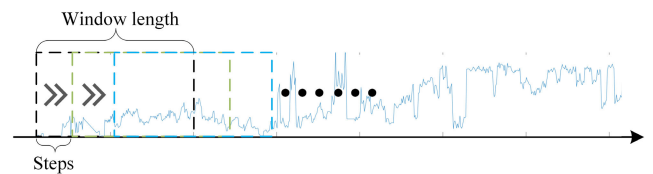


FIGURE 6. Samples of DGA monitoring data using the sliding window method.

$C_2H_6$ ,  $C_2H_2$ ,  $CO$  and  $CO_2$ . However, the majority of such devices can monitor only five gases. Hence, monitoring data for  $H_2$ ,  $CH_4$ ,  $C_2H_4$ ,  $C_2H_6$  and  $C_2H_2$  are adopted as inputs. A total of 540,000 valid entries recorded by 354 DGA online monitoring devices from 2007 to 2017 were collected (discontinuous data, zero values, infinite values and other obvious abnormal data were removed). The sliding window method was employed to build a sample base. The sliding window length was 30 days, and the step length was 5 days. As shown in Fig. 6, 102,774 valid training samples were obtained.

The computer adopted for this research is equipped with an 8-core Xeon CPU, a GTX1080 GPU and 32 GB of RAM. Notably, 441 sets of DGA online monitoring and calibration

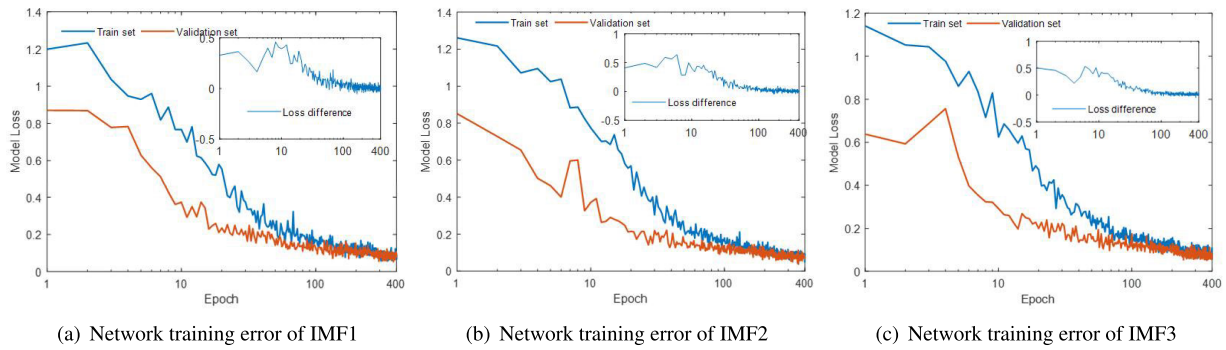


FIGURE 7. DGA signal training error Diagrams.

TABLE 1. Weight settings of source-load double-sided energy prediction tasks.

Items	Accuracy	Adjust parameters manually	Generalization performance
Method proposed in this paper	95.2%	No	Good
Method proposed in reference [4]	91.5%	No	Weak
Method proposed in reference [15]	82.3%	Yes	Weak

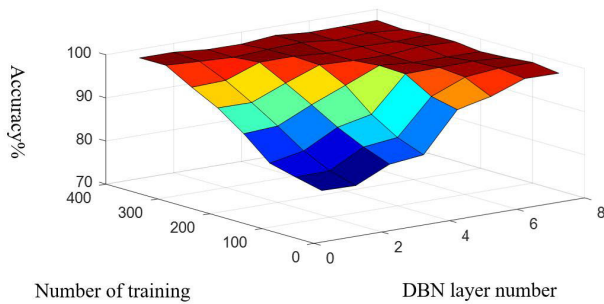


FIGURE 8. Accuracy diagram of network training for different levels of DBN.

data were retrieved from the PMS database. According to the calibration results, there were 4,541 marked samples, of which 3,632 were positive samples and 909 were negative samples. The data for various gases in the samples were decomposed. The validity evaluation network was trained using the method proposed in Chapters I and II. The signal decomposition network training error is shown in Fig. 7.

**B. COMPARISON OF DIFFERENT FEATURE EXTRACTION MODELS**

This paper adopts three network feature extraction mechanisms to test the model based on the same samples, including the DBN, RNN and FCN. The DGA data recognition precision of the evaluation models based on three types of feature extraction mechanisms is compared. The results are shown in Fig. 8.

To develop the optimal DBN structure and training parameters, this paper compares the model evaluation effects of the DGA data for different DBM layers and training cycles. Then, the optimal DBN model can be built according to the practical characteristics of the input samples.

The above figure shows that after the number of DBN model layers and number of training cycles reach 4 and 250, respectively, the model recognition precision tends to converge. At that moment, if the number of model layers or training cycles increases, the training and testing times will increase, thus decreasing the computational efficiency. In addition, considering its use in practical situations and the data analyzed in this paper, a four-layer DBN model with 250 training cycles is adopted.

The method proposed in this paper is also compared with the phase-space reconstruction method discussed in [4], [54], [55] and the black box testing and multicriteria fusion strategy given in [15], [45] to verify the validity of the method developed in this paper. The comparison results are shown in Table 1.

As shown in Table 1, the model proposed in this paper exhibits the highest precision in recognizing fault samples. Considering the weak generalization of the black box testing and multicriteria fusion strategy, the tagged value and the variable coefficient judgment criteria should be artificially selected. The validity evaluation model proposed in this paper adopts the DBN model feature extraction mechanism, which can automatically extract DGA monitoring data features under different fault and normal operation situations from mass samples. In this way, the influence caused by improper artificial feature selection can be avoided. Additionally, the generalization of the model is improved compared to that of other models.

Currently, periodical overhauling is typically adopted for the daily calibration and maintenance of DGA online monitoring devices. Due to the lack of ability to efficiently evaluate the actual operation status of monitoring devices, the maintenance and repair objects are, to some extent, random. In response to this problem, this paper proposes a strategy for

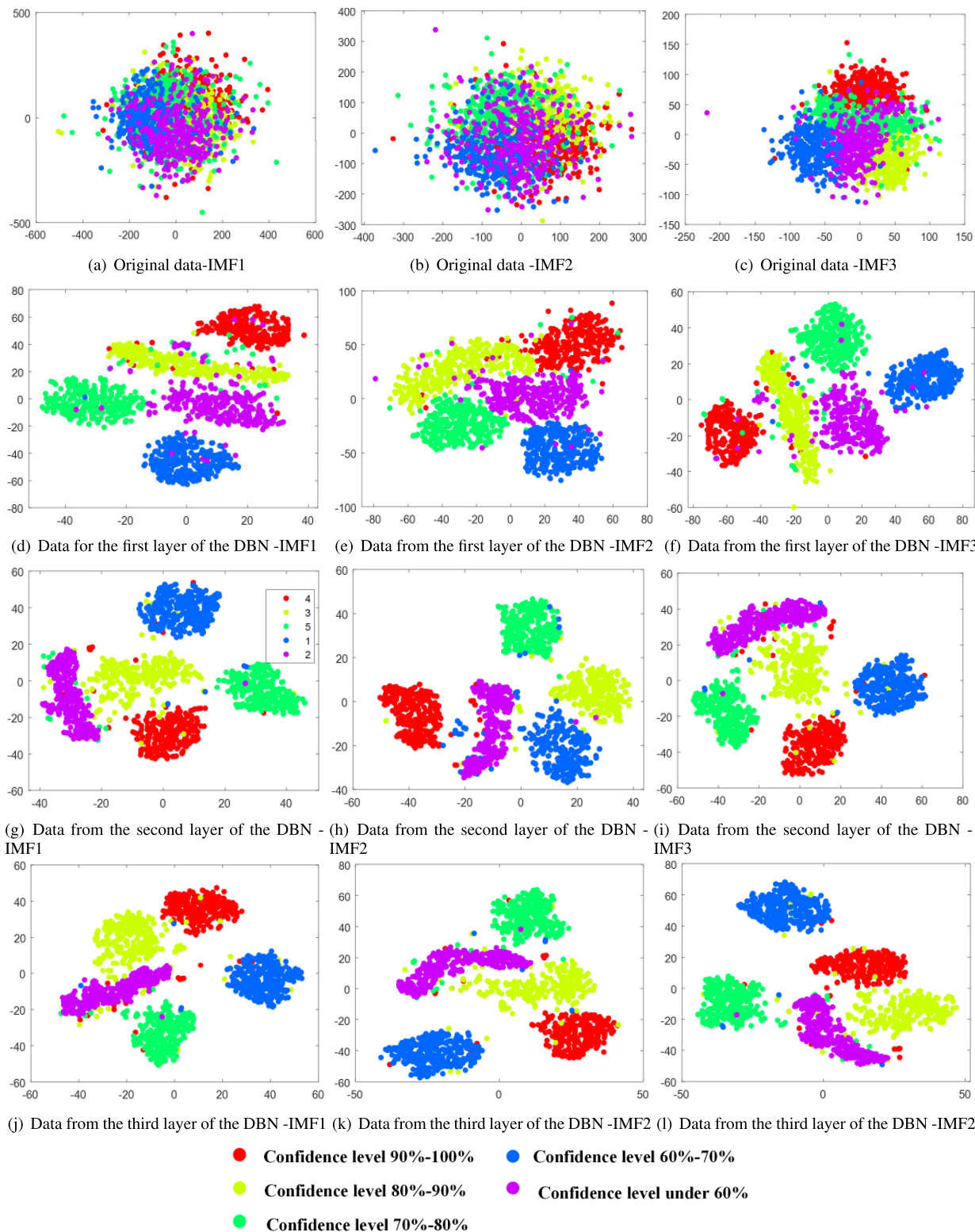


FIGURE 9. Visual comparison of t-SNE for different layers of the DBN data.

DGA device predictive maintenance. In light of the validity evaluation model, this method analyzes the health status of

the corresponding DGA devices and provides auxiliary decision making for device calibration planning.

After model decomposition and the feature extraction of DGA monitoring data via B-EMD and the DBN, this paper uses the weighting factor network to classify monitoring devices into different grades. According to the corresponding fault type of training samples and the feature vectors extracted by the model, the health status of a DGA online monitoring device is defined as follows: (1) dangerous: when the fault confidence coefficient is above 90%, repair and maintenance are necessary; (2) alarming: when the fault confidence coefficient ranges from 80% to 90%, the device should be included in the repair and maintenance plan; (3) hidden danger: the fault confidence coefficient ranges from 70% to 80%; (4) potential hidden danger: the fault confidence coefficient ranges from 60% to 70%; and (5) safe: the fault confidence coefficient is below 60%. The grade evaluation results after sample dimension reduction and the mapping of the weighting factor network are shown in Fig. 9.

#### V. PREDICTIVE MAINTENANCE OF TRANSFORMER DGA ONLINE MONITORING DEVICES

Based on the fault confidence coefficient evaluation performed by the model, this paper proposes an optimized plan for online monitoring device calibration. Below are the details of the optimization strategy.

(1) Choose the DGA monitoring data for the corresponding period according to the repair period.

Conduct data preprocessing. Remove discontinuous data, zero values, infinite values, and other obvious abnormal data. Directly include the transformer monitoring device for which the abnormal data correspond to the calibration plan.

(2) Input data into the validity evaluation model of the DGA online monitoring devices. Calculate the fault confidence coefficient of the corresponding DGA transformer in various periods of time and determine the health grade of the DGA monitoring device.

(3) Report the DGA device fault analysis results to the repair and calibration personnel to provide assistance in the implementation of the calibration plan.

(4) The optimization strategy proposed in this paper for the device calibration plan can improve the overhaul probability of DGA monitoring devices with potential hidden dangers to some extent and reduce the randomness and blindness of the maintenance schedule, thus improving the reliability of DGA online monitoring devices.

#### VI. CONCLUSION

In this paper, an EMD method for DGA signals based on B-spline interpolation and a validity analysis network for DGA data based on deep learning is proposed. This approach can effectively improve the stability of EMD at low sampling rates for DGA signals and classify the effectiveness of DGA online monitoring devices. An optimization method for the DGA calibration plan is proposed according to the validity calculation results of DGA. The experimental results demonstrate the effectiveness of the method proposed in this paper.

#### REFERENCES

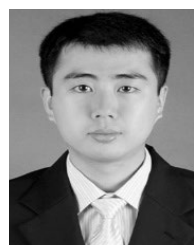
- [1] M. Duval, "Dissolved gas analysis: It can save your transformer," *IEEE Elect. Insul. Mag.*, vol. 5, no. 6, pp. 22–27, Nov. 1989.
- [2] J. L. Guardado, J. L. Naredo, P. Moreno, and C. R. Fuerte, "A comparative study of neural network efficiency in power transformers diagnosis using dissolved gas analysis," *IEEE Power Eng. Rev.*, vol. 21, no. 7, p. 71, Jul. 2001.
- [3] J. Faiz and M. Soleimani, "Dissolved gas analysis evaluation in electric power transformers using conventional methods a review," *IEEE Trans. Dielectr. Electr. Insul.*, vol. 24, no. 2, pp. 1239–1248, Apr. 2017.
- [4] P. Zhang, B. Qi, Z. Rong, and X. Li, "Optimal dissolved gas analysis data set selection based on phase space reconstruction," in *Proc. IEEE Conf. Electr. Insul. Dielectr. Phenomenon (CEIDP)*, Oct. 2017, pp. 229–232.
- [5] Q. Su, C. Mi, L. L. Lai, and P. Austin, "A fuzzy dissolved gas analysis method for the diagnosis of multiple incipient faults in a transformer," *IEEE Trans. Power Syst.*, vol. 15, no. 2, pp. 593–598, May 2000.
- [6] C. E. Lin, J.-M. Ling, and C.-L. Huang, "An expert system for transformer fault diagnosis using dissolved gas analysis," *IEEE Trans. Power Del.*, vol. 8, no. 1, pp. 231–238, Jan. 1993.
- [7] F. U. Din, A. Ahmad, H. Ullah, A. Khan, T. Umer, and S. Wan, "Efficient sizing and placement of distributed generators in cyber-physical power systems," *J. Syst. Archit.*, vol. 97, pp. 197–207, Aug. 2019.
- [8] Q. Zhang, S. Wan, B. Wang, D. W. Gao, and H. Ma, "Anomaly detection based on random matrix theory for industrial power systems," *J. Syst. Archit.*, vol. 95, pp. 67–74, May 2019.
- [9] G. Casolla, S. Cuomo, V. S. D. Cola, and F. Piccialli, "Exploring unsupervised learning techniques for the Internet of Things," *IEEE Trans. Ind. Informat.*, vol. 16, no. 4, pp. 2621–2628, Apr. 2020.
- [10] X. Wang, L. T. Yang, Y. Wang, X. Liu, Q. Zhang, and M. J. Deen, "A distributed tensor-train decomposition method for cyber-physical-social services," *ACM Trans. Cyber-Phys. Syst.*, vol. 3, no. 4, pp. 1–15, Oct. 2019.
- [11] L. Qi, X. Zhang, W. Dou, C. Hu, C. Yang, and J. Chen, "A two-stage locality-sensitive hashing based approach for privacy-preserving mobile service recommendation in cross-platform edge environment," *Future Gener. Comput. Syst.*, vol. 88, pp. 636–643, Nov. 2018.
- [12] S. Wan, Y. Zhao, T. Wang, Z. Gu, Q. H. Abbasi, and K. K. R. Choo, "Multi-dimensional data indexing and range query processing via Voronoi diagram for Internet of Things," *Future Gener. Comput. Syst.*, vol. 91, pp. 382–391, 2019.
- [13] F. Piccialli, S. Cuomo, V. S. di Cola, and G. Casolla, "A machine learning approach for IoT cultural data," *J. Ambient Intell. Hum. Comput.*, pp. 1–12, 2019.
- [14] X. Xu, R. Mo, F. Dai, W. Lin, S. Wan, and W. Dou, "Dynamic resource provisioning with fault tolerance for data-intensive meteorological workflows in cloud," *IEEE Trans. Ind. Informat.*, early access, Dec. 11, 2019, doi: 10.1109/TII.2019.2959258.
- [15] Q. Bo, P. Zhang, and R. Zhihai, "Validity assessment method of dga sensors based on data driven and multiple criterion integration," *Power Syst. Technol.*, vol. 41, no. 11, pp. 3662–3669, 2017.
- [16] M. A. Rahman, M. Y. Mukta, A. Yousuf, A. T. Asyhari, M. Z. A. Bhuiyan, and C. Y. Yaakub, "IoT based hybrid green energy driven highway lighting system," in *Proc. IEEE Int. Conf. Dependable, Auton. Secure Comput., Int. Conf. Pervas. Intell. Comput., Int. Conf. Cloud Big Data Comput., Int. Conf. Cyber Sci. Technol. Congr. (DASC/PiCom/CBDCom/CyberSciTech)*, Aug. 2019, pp. 587–594.
- [17] X. Xu, C. He, Z. Xu, L. Qi, S. Wan, and M. Z. A. Bhuiyan, "Joint optimization of offloading utility and privacy for edge computing enabled IoT," *IEEE Internet Things J.*, early access, Sep. 26, 2019, doi: 10.1109/JIOT.2019.2944007.
- [18] L. Qi, Y. Chen, Y. Yuan, S. Fu, X. Zhang, and X. Xu, "A QoS-aware virtual machine scheduling method for energy conservation in cloud-based cyber-physical systems," *World Wide Web*, vol. 23, no. 2, pp. 1275–1297, Mar. 2020.
- [19] X. Wang, L. T. Yang, H. Li, M. Lin, J. Han, and B. O. Apduhan, "NQA: A nested anti-collision algorithm for RFID systems," *ACM Trans. Embedded Comput. Syst.*, vol. 18, no. 4, pp. 1–21, Jul. 2019.
- [20] S. Ding, S. Qu, Y. Xi, and S. Wan, "Stimulus-driven and concept-driven analysis for image caption generation," *Neurocomputing*, early access, Jul. 27, 2019, doi: 10.1016/j.neucom.2019.04.095.
- [21] *Proc. Roy. Soc. London, Math., Phys. Eng. Sci.*, pp. 29–111, 1905.
- [22] W. Gong, L. Qi, and Y. Xu, "Privacy-aware multidimensional mobile service quality prediction and recommendation in distributed fog environment," *Wireless Commun. Mobile Comput.*, vol. 2018, pp. 1–8, Apr. 2018.



- [23] X. Xu, Y. Xue, L. Qi, Y. Yuan, X. Zhang, T. Umer, and S. Wan, "An edge computing-enabled computation offloading method with privacy preservation for Internet of connected vehicles," *Future Gener. Comput. Syst.*, vol. 96, pp. 89–100, Jul. 2019.
- [24] Z. Xu, B. Huang, and F. Zhang, "Improvement of empirical mode decomposition under low sampling rate," *Signal Process.*, vol. 89, no. 11, pp. 2296–2303, Nov. 2009.
- [25] A. Roy and J. F. Doherty, "Improved signal analysis performance at low sampling rates using raised cosine empirical mode decomposition," *Electron. Lett.*, vol. 46, no. 2, pp. 176–177, 2010.
- [26] Y. LeCun, Y. Bengio, and G. Hinton, "Deep learning," *Nature*, vol. 521, no. 7553, p. 436, 2015.
- [27] R. Zhang, P. Xie, C. Wang, G. Liu, and S. Wan, "Classifying transportation mode and speed from trajectory data via deep multi-scale learning," *Comput. Netw.*, vol. 162, Oct. 2019, Art. no. 106861.
- [28] S. Wan and S. Goudos, "Faster R-CNN for multi-class fruit detection using a robotic vision system," *Comput. Netw.*, vol. 168, Feb. 2020, Art. no. 107036.
- [29] Q. Chen, N. Huang, S. Riemenschneider, and Y. Xu, "A B-spline approach for empirical mode decompositions," *Adv. Comput. Math.*, vol. 24, nos. 1–4, pp. 171–195, Jan. 2006.
- [30] M. Unser, A. Aldroubi, and M. Eden, "B-spline signal processing. I. Theory," *IEEE Trans. Signal Process.*, vol. 41, no. 2, pp. 821–833, Feb. 1993.
- [31] M. A. Rahman, M. M. Hasan, A. T. Asyhari, and M. Z. A. Bhuiyan, "A 3D-collaborative wireless network: Towards resilient communication for rescuing flood victims," in *Proc. IEEE 15th Int. Conf. Dependable, Auton. Secure Comput., 15th Int. Conf. Pervas. Intell. Comput., 3rd Int. Conf. Big Data Intell. Comput. Cyber Sci. Technol. Congr. (DASC/PiCom/DataCom/CyberSciTech)*, Nov. 2017, pp. 385–390.
- [32] W. Wei, M. A. Rahman, I. F. Kurniawan, A. T. Asyhari, S. M. N. Sadat, and L. Yao, "Immune genetic algorithm optimization and integration of logistics network terminal resources," in *Proc. 3rd IEEE Int. Conf. Robot. Comput. (IRC)*, Feb. 2019, pp. 435–436.
- [33] X. Xu, Q. Liu, X. Zhang, J. Zhang, L. Qi, and W. Dou, "A blockchain-powered crowdsourcing method with privacy preservation in mobile environment," *IEEE Trans. Comput. Social Syst.*, vol. 6, no. 6, pp. 1407–1419, Dec. 2019.
- [34] H. Liu, H. Kou, C. Yan, and L. Qi, "Link prediction in paper citation network to construct paper correlation graph," *EURASIP J. Wireless Commun. Netw.*, vol. 2019, no. 1, pp. 1–12, Dec. 2019.
- [35] X. Wang, W. Wang, L. T. Yang, S. Liao, D. Yin, and M. J. Deen, "A distributed HOSVD method with its incremental computation for big data in cyber-physical-social systems," *IEEE Trans. Comput. Social Syst.*, vol. 5, no. 2, pp. 481–492, Jun. 2018.
- [36] S. Wan, Z. Gu, and Q. Ni, "Cognitive computing and wireless communications on the edge for healthcare service robots," *Comput. Commun.*, vol. 149, pp. 99–106, Jan. 2020.
- [37] H. He and E. A. Garcia, "Learning from imbalanced data," *IEEE Trans. Knowl. Data Eng.*, vol. 21, no. 9, pp. 1263–1284, Sep. 2009.
- [38] S. Wan, Y. Xia, L. Qi, Y.-H. Yang, and M. Atiqzaman, "Automated colorization of a grayscale image with seed points propagation," *IEEE Trans. Multimedia*, early access, Feb. 28, 2020, doi: [10.1109/TMM.2020.2976573](https://doi.org/10.1109/TMM.2020.2976573).
- [39] A. Salehi Fathabadi, M. J. Butler, S. Yang, L. A. Maeda-Nunez, J. Bantock, B. M. Al-Hashimi, and G. V. Merrett, "A model-based framework for software portability and verification in embedded power management systems," *J. Syst. Archit.*, vol. 82, pp. 12–23, Jan. 2018.
- [40] L. Qi, X. Zhang, S. Li, S. Wan, Y. Wen, and W. Gong, "Spatial-temporal data-driven service recommendation with privacy-preservation," *Inf. Sci.*, vol. 515, pp. 91–102, Apr. 2020.
- [41] X. Shi, Y. Zhu, C. Sa, L. Wang, and G. Sun, "Power transformer fault classifying model based on deep belief network," *Power Syst. Protection Control*, vol. 44, no. 1, pp. 71–76, 2016.
- [42] G. Qiang, Y. Wu, and L. Qian, "A faulted insulator identification algorithm of sparse difference-based deep belief network," *Elect. Meas. Instrum.*, no. 1, p. 4, 2016.
- [43] L. Xiuli, Z. Xueying, and W. Liyong, "Fault diagnosis method of wind turbine gearbox based on deep belief network and vibration signal," in *Proc. 57th Annu. Conf. Soc. Instrum. Control Eng. Jpn. (SICE)*, Sep. 2018, pp. 1699–1704.
- [44] G. M. Gu and X. Zhang, "Structural damage identification of wind turbine blade based on deep belief networks," *J. Gansu Agricult. Univ.*, no. 4, p. 22, 2016.
- [45] B. Wang, H. Ma, X. Wang, G. Deng, Y. Yang, and S. Wan, "Vulnerability assessment method for cyber-physical system considering node heterogeneity," *J. Supercomput.*, pp. 1–21, Oct. 2019, doi: [10.1007/s11227-019-03027-w](https://doi.org/10.1007/s11227-019-03027-w).
- [46] Y.-W. Zhang, Y.-Y. Zhou, F.-T. Wang, Z. Sun, and Q. He, "Service recommendation based on quotient space granularity analysis and covering algorithm on spark," *Knowl.-Based Syst.*, vol. 147, pp. 25–35, May 2018.
- [47] S. Singh and S. Tripathi, "SLOPE: Secure and load optimized packet scheduling model in a grid environment," *J. Syst. Archit.*, vol. 91, pp. 41–52, Nov. 2018.
- [48] C. Lawrence, S. Altschul, M. Boguski, J. Liu, A. Neuwald, and J. Wootton, "Detecting subtle sequence signals: A gibbs sampling strategy for multiple alignment," *Science*, vol. 262, no. 5131, pp. 208–214, Oct. 1993.
- [49] Z. Gao, Y. Li, and S. Wan, "Exploring deep learning for view-based 3D model retrieval," *ACM Trans. Multimedia Comput., Commun., Appl.*, vol. 16, no. 1, pp. 1–21, Mar. 2020.
- [50] Z. Gao, H.-Z. Xuan, H. Zhang, S. Wan, and K.-K.-R. Choo, "Adaptive fusion and category-level dictionary learning model for multiview human action recognition," *IEEE Internet Things J.*, vol. 6, no. 6, pp. 9280–9293, Dec. 2019.
- [51] N. Eltayieb, R. Elhabob, A. Hassan, and F. Li, "An efficient attribute-based online/offline searchable encryption and its application in cloud-based reliable smart grid," *J. Syst. Archit.*, vol. 98, pp. 165–172, Sep. 2019.
- [52] X. Wang, L. T. Yang, X. Xie, J. Jin, and M. J. Deen, "A cloud-edge computing framework for cyber-physical-social services," *IEEE Commun. Mag.*, vol. 55, no. 11, pp. 80–85, Nov. 2017.
- [53] F. Piccialli, G. Casolla, S. Cuomo, F. Giampaolo, and V. S. di Cola, "Decision making in IoT environment through unsupervised learning," *IEEE Intell. Syst.*, vol. 35, no. 1, pp. 27–35, Jan. 2020.
- [54] L. Qi, X. Zhang, W. Dou, and Q. Ni, "A distributed locality-sensitive hashing-based approach for cloud service recommendation from multi-source data," *IEEE J. Sel. Areas Commun.*, vol. 35, no. 11, pp. 2616–2624, Nov. 2017.
- [55] B. Wang, L. Zhang, H. Ma, H. Wang, and S. Wan, "Parallel LSTM-based regional integrated energy system multienergy source-load information interactive energy prediction," *Complexity*, vol. 2019, pp. 1–13, Nov. 2019.



**JUN JIA** is currently pursuing the Ph.D. degree in power system with Southeast University, Nanjing, China. He is working at the Research Institute, State Grid Jiangsu Electric Power Company, Ltd., Jiangsu, China. His research interests include power system online assessment, big data, integrated energy systems, and smart city.



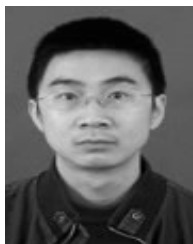
**FENGBO TAO** received the Ph.D. degree in electrical engineering from Xi'an Jiaotong University, Xi'an, China. He is working at the Research Institute, State Grid Jiangsu Electric Power Company, Ltd., Jiangsu, China. His research interests include high voltage and insulation equipment.



**GUOJIANG ZHANG** received the Ph.D. degree in electrical engineering from Zhejiang University, Hangzhou, China. He is working at the Equipment Department, State Grid Jiangsu Electric Power Company, Ltd. His research interests include power system online assessment and big data.



**JIN SHAO** received the master's degree in electrical engineering from Chongqing University, Chongqing, China. He is working at the Equipment Department, State Grid Corporation of China, Ltd. His research interests include high voltage and insulation equipment.



**BO WANG** received the Ph.D. degree in computer science from Wuhan University, Wuhan, China, in 2006. He was a Postdoctoral Researcher with the School of Electrical Engineering, Wuhan University, from 2007 to 2009. He is currently an Associate Professor with the School of Electrical Engineering, Wuhan University. His research interests include power system online assessment, big data, integrated energy systems, and smart city.

• • •



**XINGHUI ZHANG** received the master's degree in electrical engineering from Southeast University, Nanjing, China. He is working at the Equipment Department, State Grid Corporation of China, Ltd. His research interests include power system online assessment and big data.